ELSEVIER

Ceramics International 32 (2006) 73–83

CERAMICS INTERNATIONAL

www.elsevier.com/locate/ceramint

Effect of strontium concentration on electrical conduction properties of Sr-modified $BaSnO_3$

Ashok Kumar [a], R.N.P. Choudhary [b,*], B.P. Singh [a], Awalendra K. Thakur [b]

[a] *Department of Physics, T.M. Bhagalpur University, Bhagalpur, India*
[b] *Department of Physics and Meteorology, Indian Institute of Technology, Kharagpur-721302, India*

Received 8 June 2004; received in revised form 18 October 2004; accepted 21 December 2004
Available online 7 March 2005

Abstract

Strontium-substituted barium stannate having a general formula $Ba_{1-x}Sr_xSnO_3$ ($0 \leq x \leq 0.15$) has been prepared by a high-temperature solid-state reaction method. The formation of the materials has been confirmed by X-ray diffraction study. A preliminary analysis of XRD data indicates a cubic unit cell as the best fit for both pure and Sr-substituted $BaSnO_3$.The strontium substitution has resulted into modification of sample microstructure evidenced by textural changes and enhancement in the sample porosity evaluated using XRD data. The surface morphology investigated by scanning electron microscopy reveals a polycrystalline texture and a porous microstructure that has been found to increase with increase in strontium concentration.The effect of microstructural changes on doping has resulted in a modification of the electrical properties. Electrical properties investigated using impedance analysis technique indicate (i) presence of negative temperature coefficient of resistance (NTCR) behaviour that is also retained on doping (ii) evidences of single electrical relaxation attributed to the presence of bulk contribution to the electrical properties, (iii) presence of temperature dependent electrical relaxation phenomenon and (iv) an enhancement in the barrier to the mobility of charge carrier on Sr-substitution. Electrical conductivity has been found to increase substantially at higher temperature (>300 °C) and it may be attributed possibly to the oxygen vacancies. Conductivity spectrum analysis suggests the hopping of charge carrier among localized site as the possible mechanism for electrical conduction. The effects of Sr concentration on changes in the electrical conductivity as a function of temperature and frequency are described based on impedance spectrum analysis.

Keywords: B. Microstructure; C. Impedance; C. Electrical properties; C. Electrical conductivity

1. Introduction

Cubic perovskite (ABO_3) type pure stannates having a general formula $MSnO_3$ (M = Ba, Ca, Sr) have been well studied for their formation, optimization of preparation methods and structural analysis [1–10]. It has been observed that a partial substitution of cations at M/Sn sites results in substantial modification in their physical properties so as to make them suitable for a wide variety of industrial applications. $BaSnO_3$, belonging to the family of the perovskite, is of particular interest from both fundamental and materials technology point of view due to its unusual dielectric and semi-conducting properties. This material has been found to be interesting for a number of applications in industry such as; a glass enamel to improve alkali resistance, a component of dielectric ceramics, a multi-functional signal sensor to detect temperature, humidity and gas, as a negative electrode active material for long life energy storage application and in the fabrication of ceramic boundary-layer capacitors, etc. [11–14].

Literature survey reveals that alkaline earth-based stannates and their modified forms (i.e., substitution/mixed combination) are important electronic ceramics in view of their interesting physical properties. A detailed studies on different aspects of physical properties such as crystal structure, thermodynamical properties, electronic disorder, sensing properties and dielectric properties on various type of stannates have already been reported in literature. Substitution at the M/Sn site in the stannates result in

* Corresponding author. Tel.: +91 3222 283814.
E-mail address: crnpfl@phy.iitkgp.ernet.in (R.N.P. Choudhary).

0272-8842/$30.00
doi:10.1016/j.ceramint.2004.12.010

noticeable modification in their microstructure leading ultimately to the tailoring of their physical properties [15–17]. The effect of M site substitution in different stannates by transition metal (Co, Cr)/rare earth metal (La) has been reported and changes in the physical properties of the corresponding modified stannates has been reported [18–19]. However, the effect of Ba substitution in $BaSnO_3$ by Sr (a slightly bigger member of the same group) has not been studied as yet. Further, since structural/microstructural changes in a system drastically modify their physical properties, a detailed study of electrical properties of M/Sn site-substituted stannates assumes greater significance in order to have a complete picture of the electrical behaviour of semiconducting stannate-based ceramics. A survey shows that electrical properties of Ba/Sn site-substituted $BaSnO_3$ (with La at barium site and Co, Cr at the Sn site) has been reported [18,19]. However, the effect of concentration over a wide range of doping concentration on their electrical properties has not been studied.

This aspect has motivated us to undertake the present work comprising of a detailed analysis of the effect of dopant concentration on electrical properties of Sr-modified $BaSnO_3$. The present paper aims to report an analysis of the electrical properties of Sr-substituted $BaSnO_3$ in different Sr/Ba ratio over a range of concentration ($x = 0$, 0.05, 0.10, 0.15) using complex impedance spectroscopy (CIS) technique. The CIS approach of analyzing electrical properties gives an unambiguous result over a range of temperature and frequencies. The results are basically independent of sample geometrical factors and enable us to establish a correlation of the electrical properties with the sample microstructure.

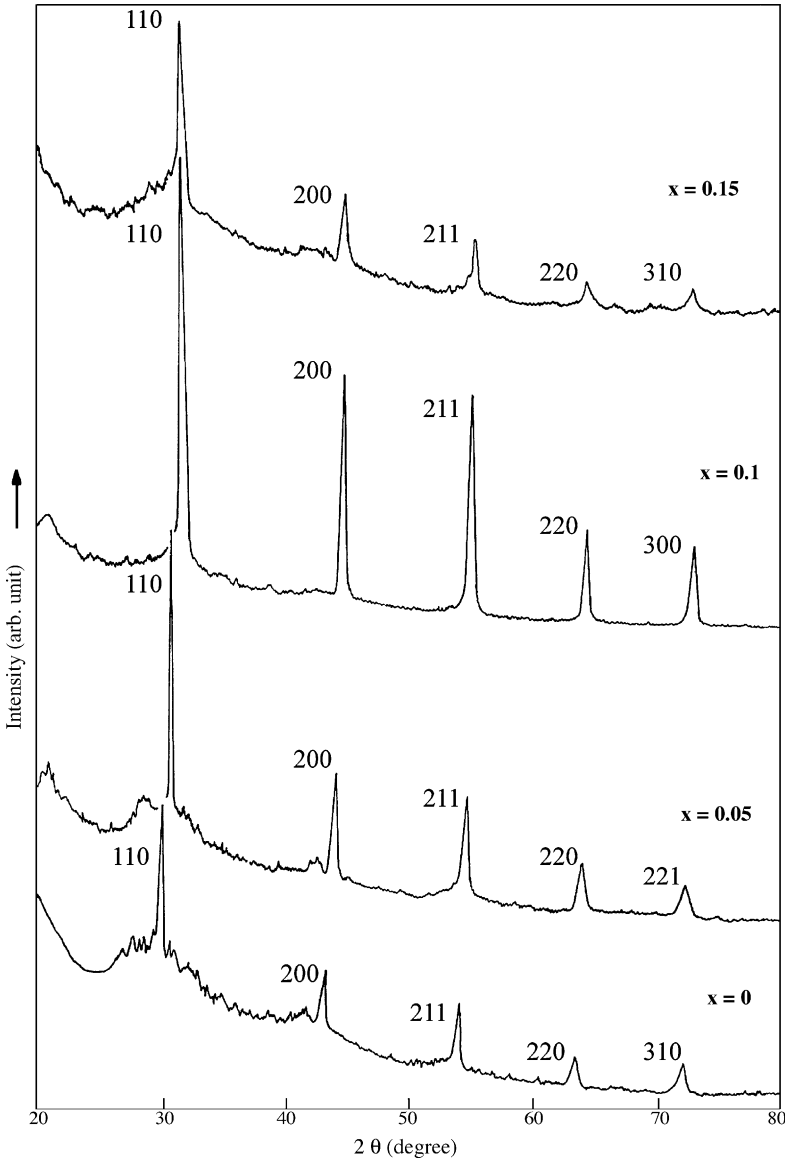

Fig. 1. XRD pattern of $Ba_{1-x}Sr_xSnO_3$ ($x = 0$–0.15) at room temperature.

Table 1
Unit cell properties of $Ba_{1-x}Sr_xSnO_3$ based on XRD data

Serial number	Material properties	Sr concentration, x (%)			
		0	5	10	15
1	Unit cell parameter (Å)	$a = 4.1591 \pm 0.0307$	$a = 4.0024 \pm 0.0019$	$a = 4.0164 \pm 0.0055$	$a = 4.1529 \pm 0.0014$
2	Unit cell volume (Å^3)	71.93	64.12	64.79	71.62
3	Theoretical density (g/cc)	7.01	7.80	7.66	6.87
4	Observed (bulk) density (g/cc)	5.80	5.76	5.26	4.66
5	Porosity (%)	23	26	31	32

2. Experimental procedure

Appropriate stoichiometric ratio of the precursors ($BaCO_3$, $SrCO_3$ and SnO_2) of high purity were weighed and initially mixed mechanically in an agate mortar for 2 h. Subsequently, it was calcined in an alumina crucible at 1000 °C for 12 h. The calcined powder was thoroughly mixed again and recalcined at 1200 °C for 12 h. The calcined powder so obtained was cold pressed into cylindrical pellets of diameter 10 mm and thickness 1–2 mm with polyvinyl alcohol (PVA) as the binder, using a hydraulic press at a pressure of $\sim 3 \times 10^7$ kg m^{-2}. The pellets were then sintered in an air atmosphere at 1200 °C for 12 h, and then polished with fine emery paper to make their faces flat and parallel. The pellets were finally coated with conductive silver paint and dried at 150 °C for 2 h before carrying out impedance measurements.

X-ray diffraction (XRD) data of the materials were obtained in the wide range of Bragg angles (2θ) (20–80°) at a scan speed of 2° min^{-1} by an X-ray diffractometer (Miniflux, Rikagu, Japan) using CuKα radiation (λ = 1.5418 Å) at room temperature. Scanning electron micrographs of the materials were taken with high-resolution scanning electron microscope (SEM: JOEL-JSM, model: 5800F) to study the surface morphology/microstructure of the sample pellets. The sample pellets were gold coated prior to being scanned under high-resolution field emission gun of SEM. The gold coating was carried out under argon (Ar) atmosphere at a vacuum of $\sim$1.33 N/m^2. The impedance studies were carried out at an input signal level of 1.3 V in the temperature range of 35–500 °C using a computer-controlled impedance analyzer (HIOKI LCR Hi TESTER, model: 3532) in the frequency range of 100 Hz to 1 MHz.

3. Results and discussion

X-ray diffraction studies have been carried out to confirm the formation of the material. Fig. 1 represents the XRD pattern of $Ba_{1-x}Sr_xSnO_3$ for different concentration of strontium (x = 0, 0.05, 0.10, 0.15). The sharp and single diffraction peaks that are different from those of the precursor materials confirm the formation of single-phase polycrystalline $Ba_{1-x}Sr_xSnO_3$ materials. The XRD pattern of $BaSnO_3$ matches well with the previous reports [1–5,20]. The XRD patterns of the Sr-substituted material (i.e., $Ba_{1-x}Sr_xSnO_3$) has been observed to be similar to that of $BaSnO_3$ except for a very small shift in the peak positions that has been noticed after partial substitution of barium (Ba) by various concentration (x = 0.05, 0.1, 0.15) of strontium (Sr). The XRD peaks have successfully been indexed using standard computer software POWDMULT [20]. Preliminary structural analysis has indicated that the unit cell of $Ba_{1-x}Sr_xSnO_3$ still remains cubic with an insignificant change in the lattice parameter (a) depending on Sr concentrations. The lattice parameter of the compound was refined by the least-squares refinement method and is shown in Table 1. The slight changes in the unit cell volume and lattice parameter with Sr concentration may possibly be attributed to a change in the chemical environment of the material resulting in a modification in their microstructure. The XRD data has been used to evaluate the theoretical density of the material and compared with its measured density. These values gave an estimate of the porosity of the sample pellet. The density and porosity data for different Sr-modified materials are also given in Table 1. It appears that replacement of Ba by Sr in $BaSnO_3$ results in an enhancement of porosity. The value of the porosity increases with increasing concentration of Sr under the reported conditions of sample preparation. This may possibly be affecting sample microstructure.

Figs. 2a–d show the scanning electron micrographs of the materials describing their surface property and microstructure. The micrographs reveal a polycrystalline nature of the material with porous microstructure. The granular size appears to change and the number of voids has been found to increase with increasing concentration of Sr. This result is in good agreement with the observations made from XRD studies for different Sr concentrations x (0–15%). The texture of the material appears to be gradually modified on substitution of Sr at the M-site (Figs. 2a–d). The grain size of $BaSnO_3$ has been estimated in the range of 2–6 μm and it gets substantially modified with increasing concentration of Sr.

The electrical properties of the materials have been studied using a complex impedance spectroscopy (CIS) technique with an objective to understand the changes in electrical properties of the materials over a wide range of frequency and temperature as a function of dopant concentration. Fig. 3a (parts i–iv) show complex impedance spectrum (Nyquist plot) for different Sr concentration over a

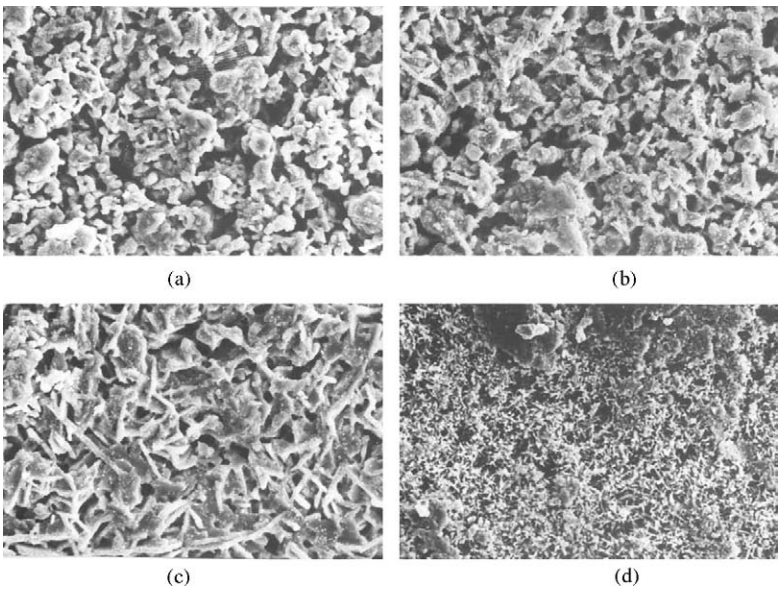

Fig. 2. Scanning electron micrographs of $Ba_{1-x}Sr_xSnO_3$ ($x = 0$–0.15).

range of temperature. The impedance spectrum is characterized by the appearance of a single semicircular arc whose radii of curvature decreases with increasing temperature. The intercept of semicircular arc with the real axis (Z'-axis) gives an estimate of sample resistance (frequency independent impedance). It has been observed that sample resistance decreases with rise in temperature, which may be related to the negative temperature coefficient of resistance (NTCR) behavior typical to a semiconductor. It also appears that the impedance increases even for a very small concentration of Sr sample (5%) when compared with that of pure $BaSnO_3$ sample irrespective of temperature. Further, as Sr-concentration increases the impedance gradually tends to decrease with rise in temperature obeying the NTCR behaviour. This result may be interpreted as an enhancement in the barrier to the mobility of charge carrier on Sr-doping accompanied by retention of typical semiconducting properties. It also suggests that the energy of activation for the mobile charge carrier may possibly increase with Sr-doping in $BaSnO_3$.

The appearance of single semicircle in the impedance pattern at all temperature suggests that the electrical processes occurring in the material has a single relaxation possibly due to the contribution from bulk material (grain interior properties). It also indicates complete absence of grain boundary effects in Sr-doped $BaSnO_3$ (Ba replaced by Sr) which is typically different from impedance result of transition metal-substituted $BaSnO_3$ (at Sn site) where grain boundary conduction has also been observed [19]. An electrical behaviour of this type may be represented, in terms of an equivalent circuit, as comprising of a parallel combination of bulk resistance (R_b) and bulk capacitance (C_b) shown in Fig. 3a (part v). These results further suggest that principal charge (current) carrier in the material may possibly be either electron or oxygen vacancies [21,22]. Lu et al. [5] have already provided the evidence of oxygen ion conduction in $BaSnO_3$ at elevated temperatures.

Fig. 3b represents the impedance loss spectrum (i.e., variation of imaginary part of impedance (Z'') with frequency) that provides an insight into the electrical processes having the largest resistance in accordance with relations:

$$Z' = R\left[\frac{\omega RC}{1+(\omega RC)^2}\right], \qquad Z'' = R\left[\frac{(\omega RC)^2}{1+(\omega RC)^2}\right]$$

The pattern of variation is characterized by: (a) the appearance of peaks at a particular frequency at each temperature for both the pure and Sr-doped $BaSnO_3$, (b) a decrease in the height of the peaks with rise in temperature, (c) significant broadening of the peaks with rise in temperature (d) marked asymmetry in the peak pattern and (e) merger of the spectrum at higher frequencies irrespective of temperature. Broadening of the peaks with rise in temperature suggests the presence of temperature dependent relaxation process in the material. The asymmetric broadening of the peaks suggests the presence of electrical processes in the material with spread of relaxation time (indicated by peak width) with two equilibrium portions. The relaxation species may possibly be electrons/immobile species at low temperature and defects at higher temperature that may be responsible for electrical conduction in the material by hopping of electrons/oxygen ion vacancy among the available localized sites [5,19]. Further, the magnitude of Z'' decreases with a shift in the peak frequency towards the higher frequency side with rise in temperature. This type of impedance spectrum arises probably due to the presence of space charge in the material. The effect of Sr substitution at the Ba-site in different proportions is quite significant as indicated by the changes in the pattern of loss spectrum for different compositions of

Sr when compared with the pattern for pure $BaSnO_3$ ($x = 0$). The peaks in loss spectrum appear to shift towards low frequency side with the addition of Sr. These peaks in the spectra, attributed to a phenomenon related to minimum capacitive effect, has been observed to shift towards lower frequency domain on addition of Sr indicating an enhancement in the net impedance of the substituted materials thereby enhancing the barrier properties in the material. It is in good agreement with the observations made from complex impedance plots (Fig. 3a). Further, the capacitive effect at a particular temperature has been observed to be higher in the $BaSnO_3$ than in the case of substituted one. These effects may possibly be related to the modification in the microstructure, crystal imperfections, and volume changes in the material on substitution as observed in XRD. In addition, the magnitude of Z'' decreases gradually with a shift in the peak frequency towards the high frequency side finally merging in the high frequency domain,

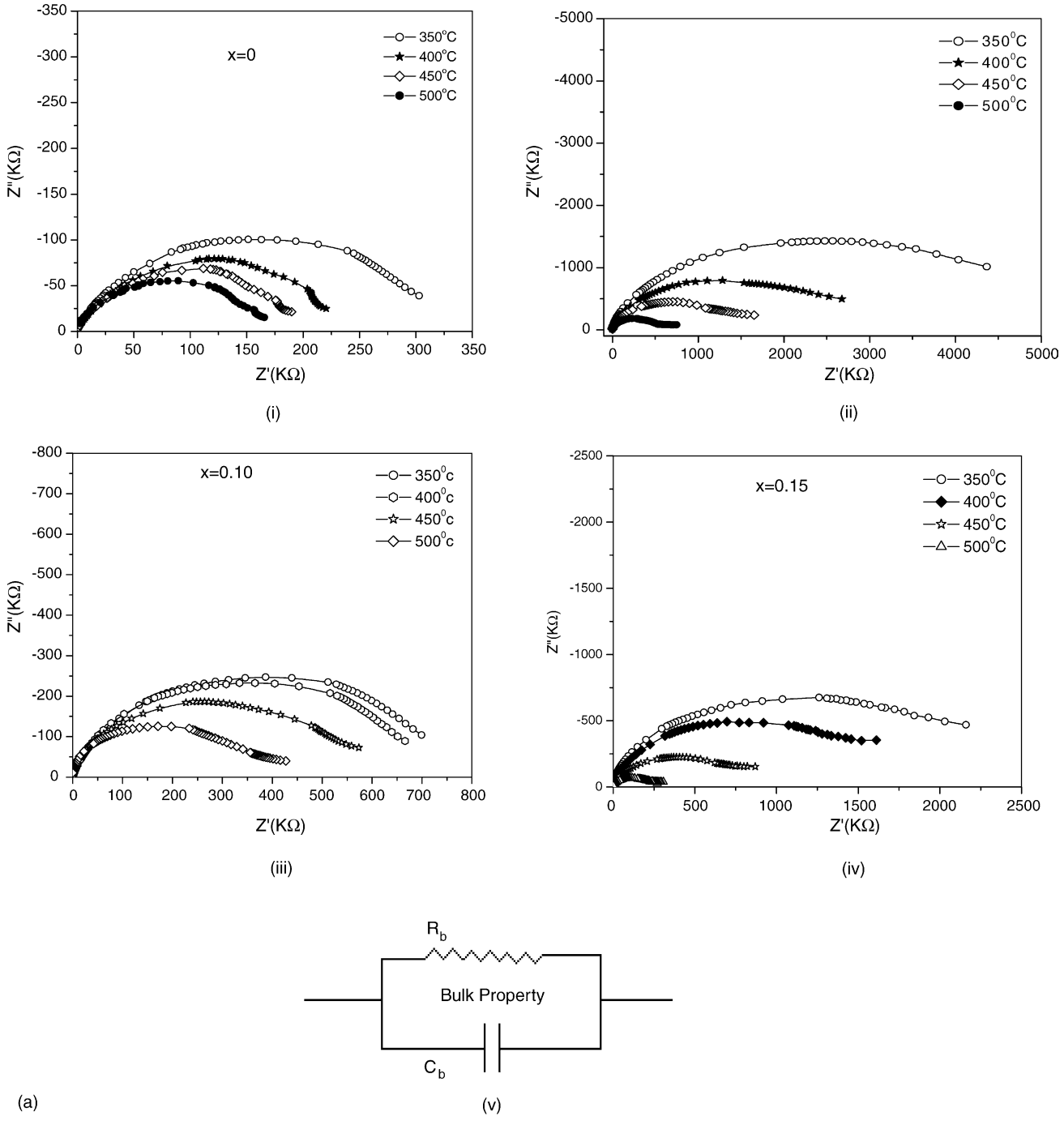

Fig. 3. (a) Complex impedance spectrum (Nyquist plot) of $Ba_{1-x}Sr_xSnO_3$ ($x = 0$–0.15), (b) loss spectrum (Z'' vs. frequency plot) of $Ba_{1-x}Sr_xSnO_3$ ($x = 0$–0.15), and (c) relaxation time ($\ln \tau$) as a function of temperature of $Ba_{1-x}Sr_xSnO_3$ ($x = 0$–0.15).

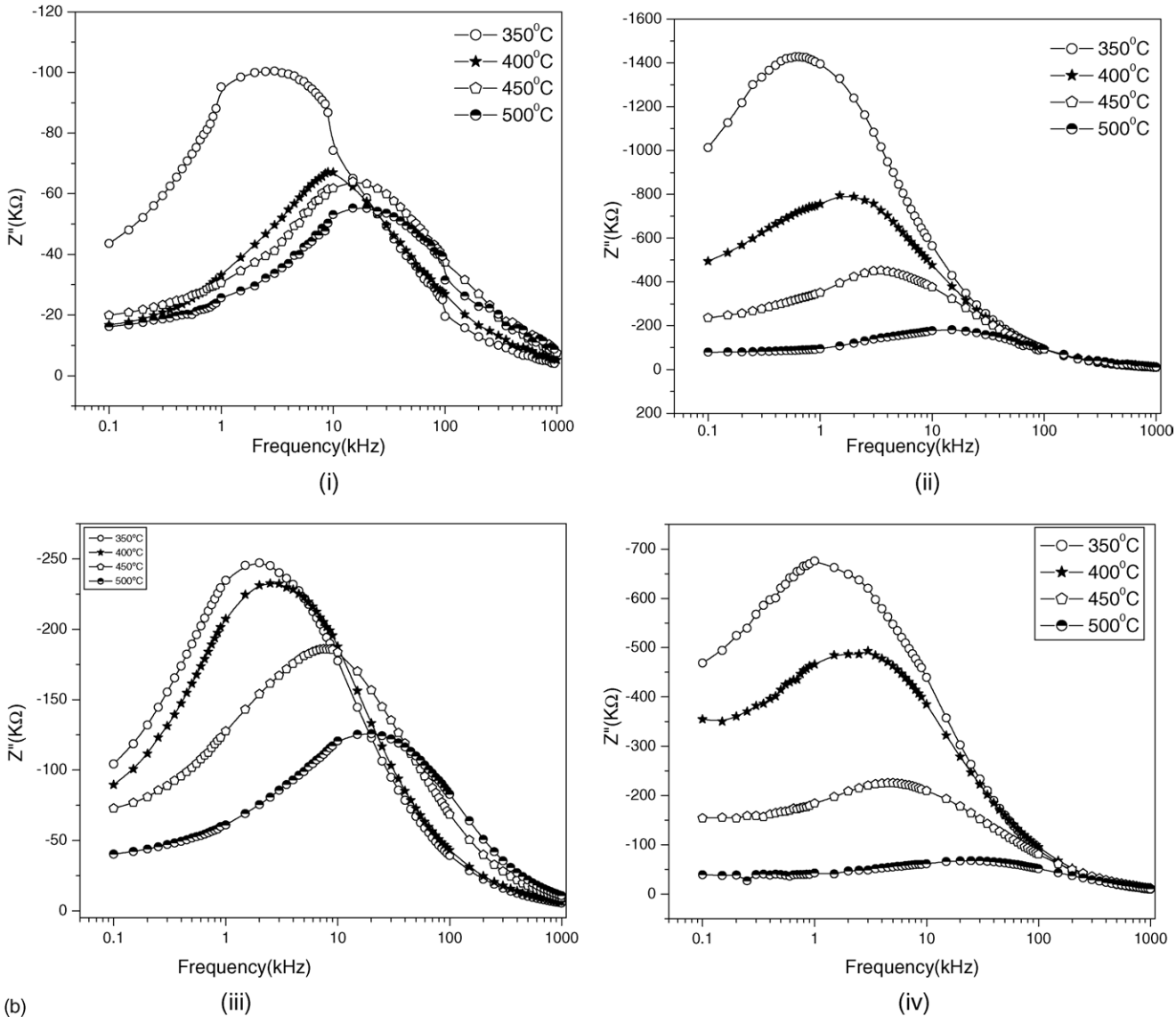

Fig. 3. (*Continued*)

irrespective of temperature. This trend is almost similar for all the concentration. This behavior of the loss spectra possibly provides an indication of the evidence of space charge in the material that governs electrical processes in the region of high frequencies.

The impedance data has been used to evaluate the relaxation time of the electrical phenomena in the material at different temperature and plotted as a function of temperature (Fig. 3c). The value of relaxation time (τ) calculated using the relation, $\omega_{max}\tau = \omega_{max}R_bC_b = 1$, is independent of the geometrical shape and size of the material but dependent only on the characteristic properties of the material. The typical variation in the pattern shows a steady increase in relaxation time with gradual change of slope in different temperature regions. This implies that electrical relaxation may possibly be due to the migration of charged species/defects. The result also indicates that the relaxation time of the conducting species lies in the range of 10 μs to 1 ms over a range of temperature from 300 °C to 500 °C. The trend of variation for all the composition is almost similar. These observations suggest the presence of temperature dependent relaxation process in the material with a spread of relaxation time in close agreement with the observations from Fig. 3a and b. The temperature dependence of (τ) may be approximated to a linear behaviour of Arrhenious type governed by the relation: $\tau = \tau_o e^{-E_a/KT}$. The activation energy (E_a) evaluated for each concentration of dopant is shown in Table 2. The energy of activation of the material has been found to increase on Sr addition in close agreement with the impedance spectrum observations.

Fig. 4a shows the variation of dc electrical conductivity (σ_{dc}) evaluated from impedance spectrum as a function of temperature for different concentration of Sr. The effect of

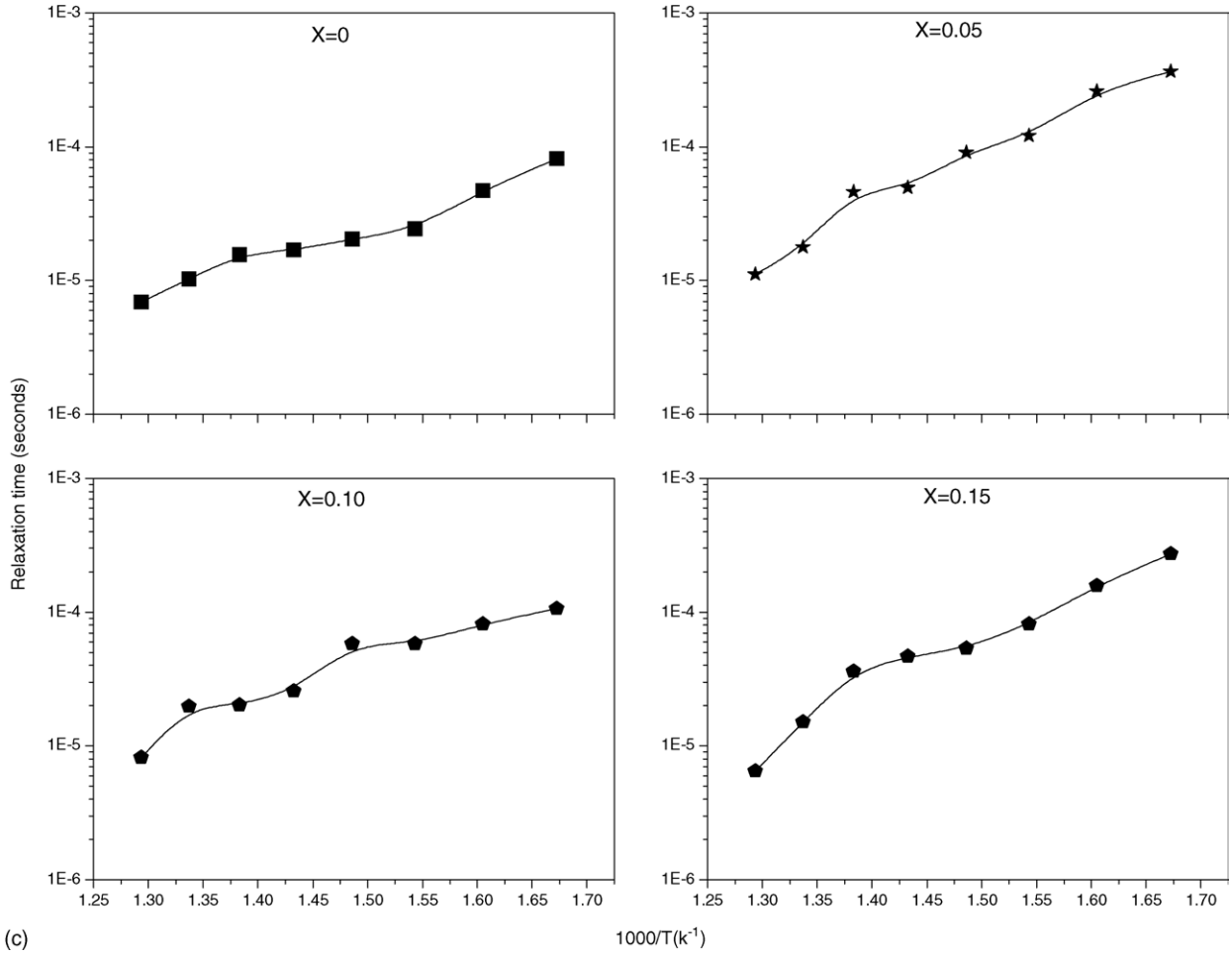

Fig. 3. (*Continued*).

Table 2
Electrical properties of $Ba_{1-x}Sr_xSnO_3$ based on impedance measurements

$Ba_{1-x}Sr_xSnO_3$, x (%)	Direct current conductivity (σ_{dc})			Activation energy	
	RT	300 °C	500 °C	E_τ (eV)	E_σ (eV)
0	1.61×10^{-8}	1.09×10^{-6}	3.11×10^{-6}	0.51	0.23
5	8.45×10^{-10}	3.47×10^{-8}	6.23×10^{-7}	0.78	0.59
10	8.08×10^{-8}	5.85×10^{-7}	1.75×10^{-6}	0.55	0.29
15	9.68×10^{-8}	2.15×10^{-7}	2.29×10^{-6}	0.69	0.44

Sr substitution is clearly reflected in the pattern (σ_{dc} versus T). It indicates a typical Arrhenius type thermally activated process for all the concentration of Sr obeying the relation, $\sigma = \sigma_o\, e^{-E_a/KT}$, where σ_0 = pre exponential factor, E_a = activation energy, K = Boltzmann constant electrical conductivity for all the compositions have been observed to increase with rise in temperature with 1–2 orders of jump at 300 °C after which there is no substantial increase (except by a factor of 2–3). The σ_{dc} values at selected temperatures are shown in Table 2 for comparison. The Arrhenius plot has been used to estimate the activation energy of the materials and are recorded in Table 2. This value of activation energy (E_a), when compared with the activation energy values (E_τ) shows marked differences for each concentration. This result possibly provides an indication that electrical species (charge carriers) involved in the process of relaxation and conduction are different.

The variation of σ_{dc} as a function of Sr concentration at different temperatures is shown in Fig. 4b. The typical behavior of electrical conductivity appears to be almost similar at different temperatures in the present study with a characteristic dip at $x = 0.05$ followed by a gradual increase onwards at higher x values. This pattern is also reflected in the variation of activation energy values of ($Ba_{1-x}Sr_xSnO_3$) from $x = 0$ to 0.15. The characteristic decrease in the dc conductivity by ~2 orders of magnitude for $x = 0.05$ at RT and 300 °C (Table 2) may possibly be attributed purely to the effect of Ba replacement by Sr in the sample. It may be related to an enhancement in the barrier properties of the material on Sr doping due to modification in microstructure/changes in volume on substitution to a certain degree. However, it requires further investigation at the microscopic level by vibrational spectroscopy techniques.

The variation of ac conductivity of ($Ba_{1-x}Sr_xSnO_3$) as a function of frequency at different temperatures is shown in

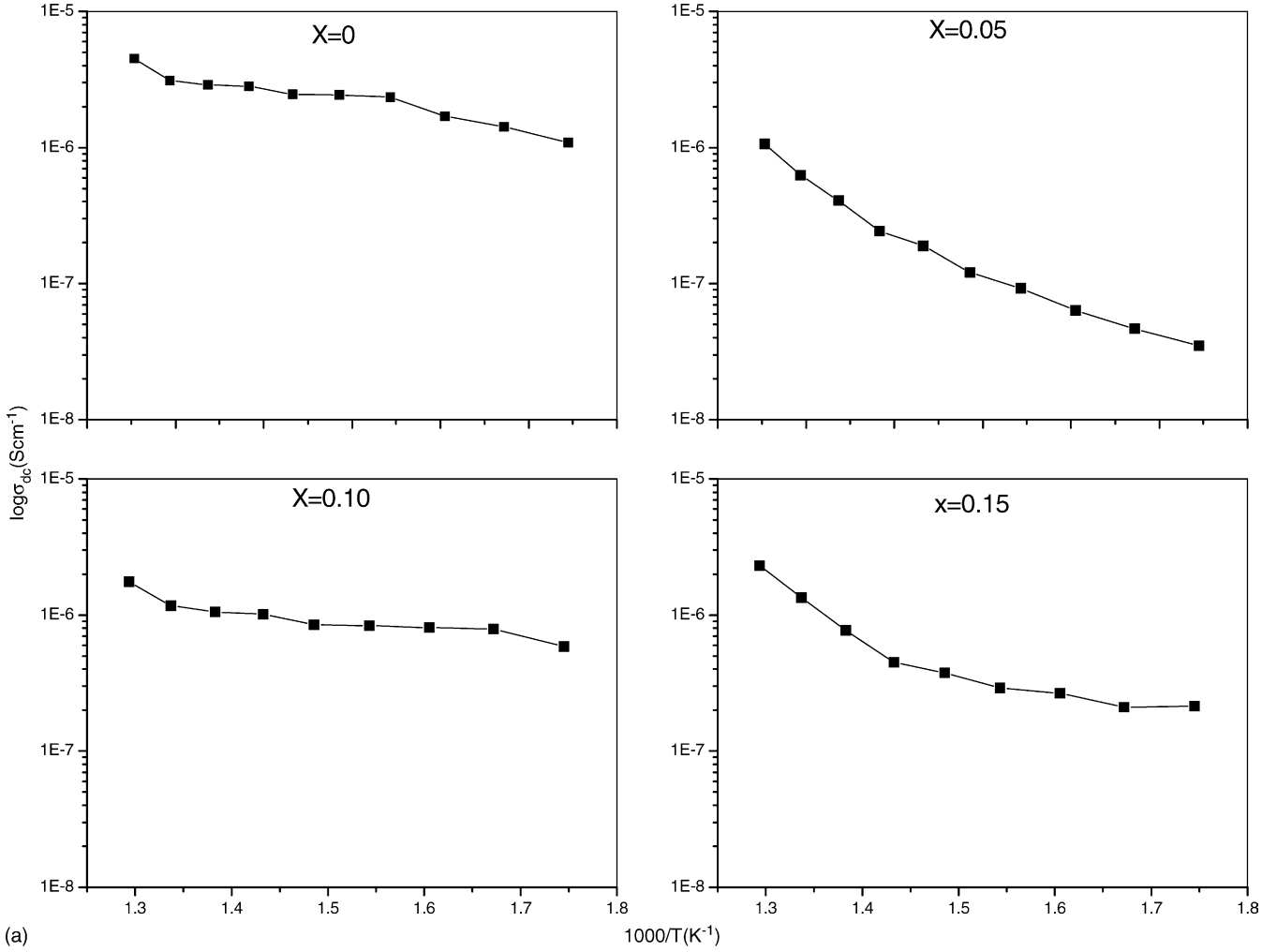

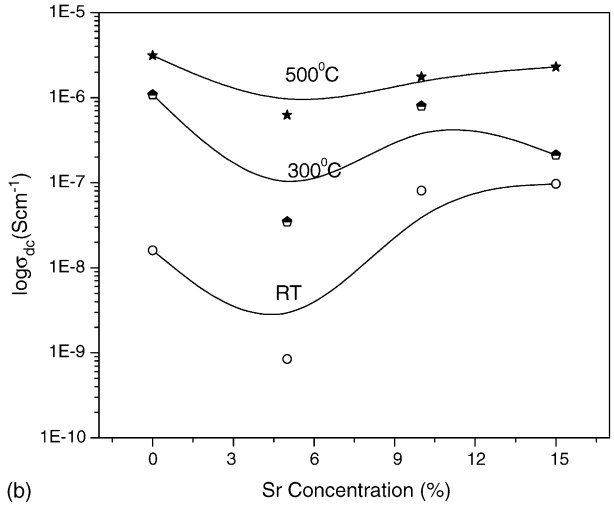

Fig. 4. (a) Variation of dc electrical conductivity of $Ba_{1-x}Sr_xSnO_3$ ($x = 0$–0.15) as a function of temperature and (b) variation of dc electrical conductivity of $Ba_{1-x}Sr_xSnO_3$ ($x = 0$–0.15) as a function of strontium concentration.

Fig. 5a (parts i–iv) for different concentrations of Sr ($x = 0$, 0.05, 0.10, and 0.15). The pattern of conductivity spectrum shows typical features of: (i) dispersion throughout the frequency range of investigation up to a temperature of 300 °C starting from room temperature, (ii) low frequency plateau and high frequency dispersion with a change in slope at higher temperature (>300 °C) and (iii) closeting behaviour of the spectrum at higher temperatures in the high frequency

region irrespective of temperature values. Further, ac conductivity pattern at higher temperature tends to merge and approach closer to each other in the high frequency range. These results indicate the existence of multiple relaxation and thermally activated process in close agreement with the observations from impedance spectrum results.

The appearance of conductivity dispersion at lower temperatures (i.e., room temperature to 300 °C) suggests that electrical conduction in material is a thermally activated process. As temperature rises (above 300 °C), the pattern of conductivity variation with frequency shows a low frequency conductivity plateau followed by high-frequency conductivity dispersion with a change in slope. The frequency at which change in slope of the pattern occurs is known as hopping frequency (ω_p). These results suggest that electrical conduction in the material takes place via hopping mechanism governed by the Jonscher's universal power law: $\sigma_{ac} = \sigma_{dc} + A\omega^n$ where A is a thermally activated constant depending upon temperature. The dispersion at lower temperature possibly indicates the presence of space charge in the material that vanishes at higher frequency and temperatures.

Fig. 5b shows the variation of σ_{ac} as a function of Sr concentration at different temperature and frequencies. The typical variation has almost similar trend as that of σ_{dc} versus Sr concentration shown in Fig. 4b with a characteristic dip at a Sr concentration of 5%. This result indicates that the nature of electrical transport (conduction) in the material is governed basically by Sr concentration, the nature being similar at every frequency at a particular temperature. This result provides an indication that the electrical behavior is predominantly dependent upon the level of substitution at the Ba-site of the $BaSnO_3$ and the lowering in conductivity

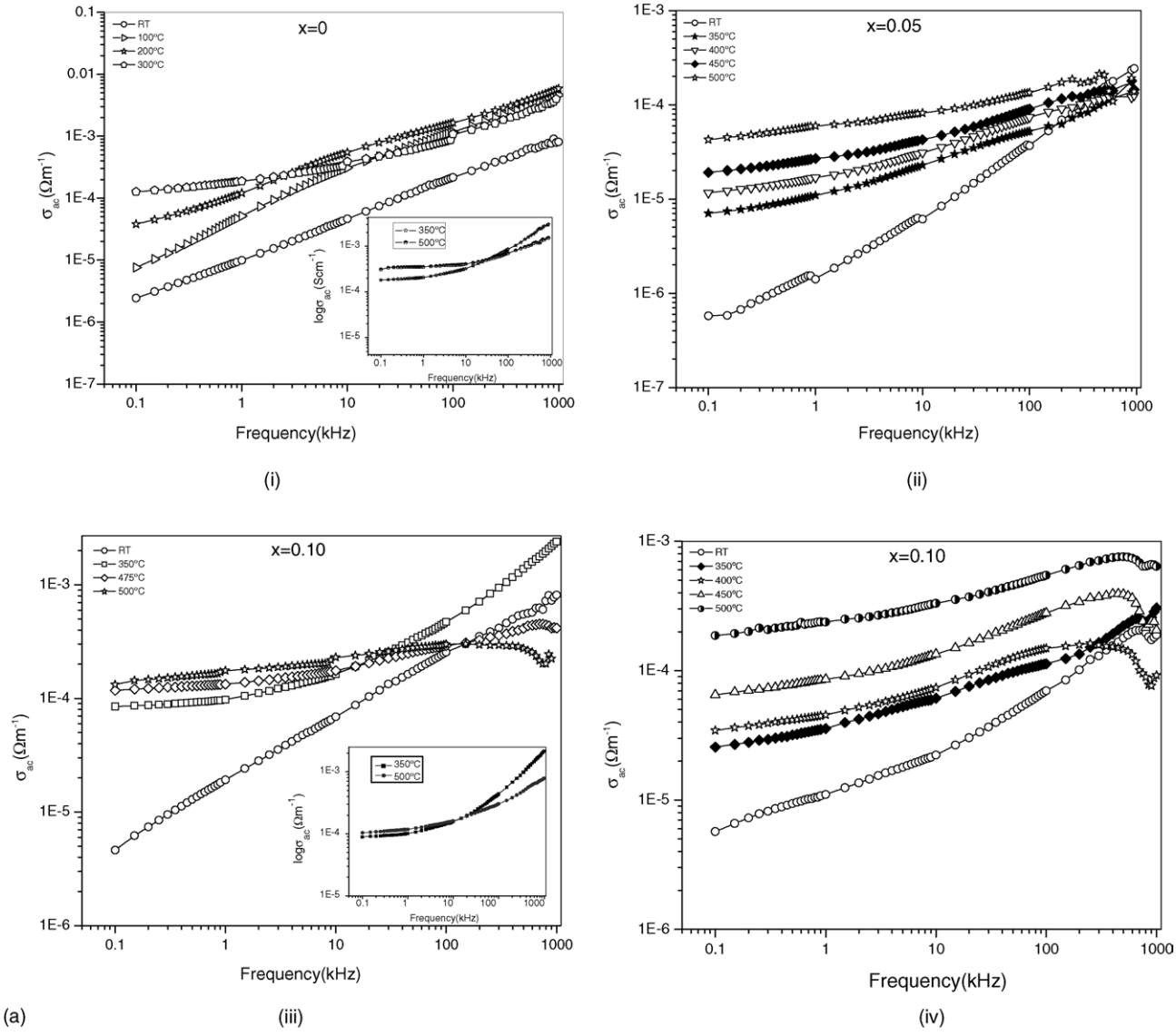

Fig. 5. (a) Variation of ac electrical conductivity of $Ba_{1-x}Sr_xSnO_3$ (x = 0–0.15) as a function of frequency and (b) variation of ac electrical conductivity of $Ba_{1-x}Sr_xSnO_3$ (x = 0–0.15) as a function of strontium concentration.

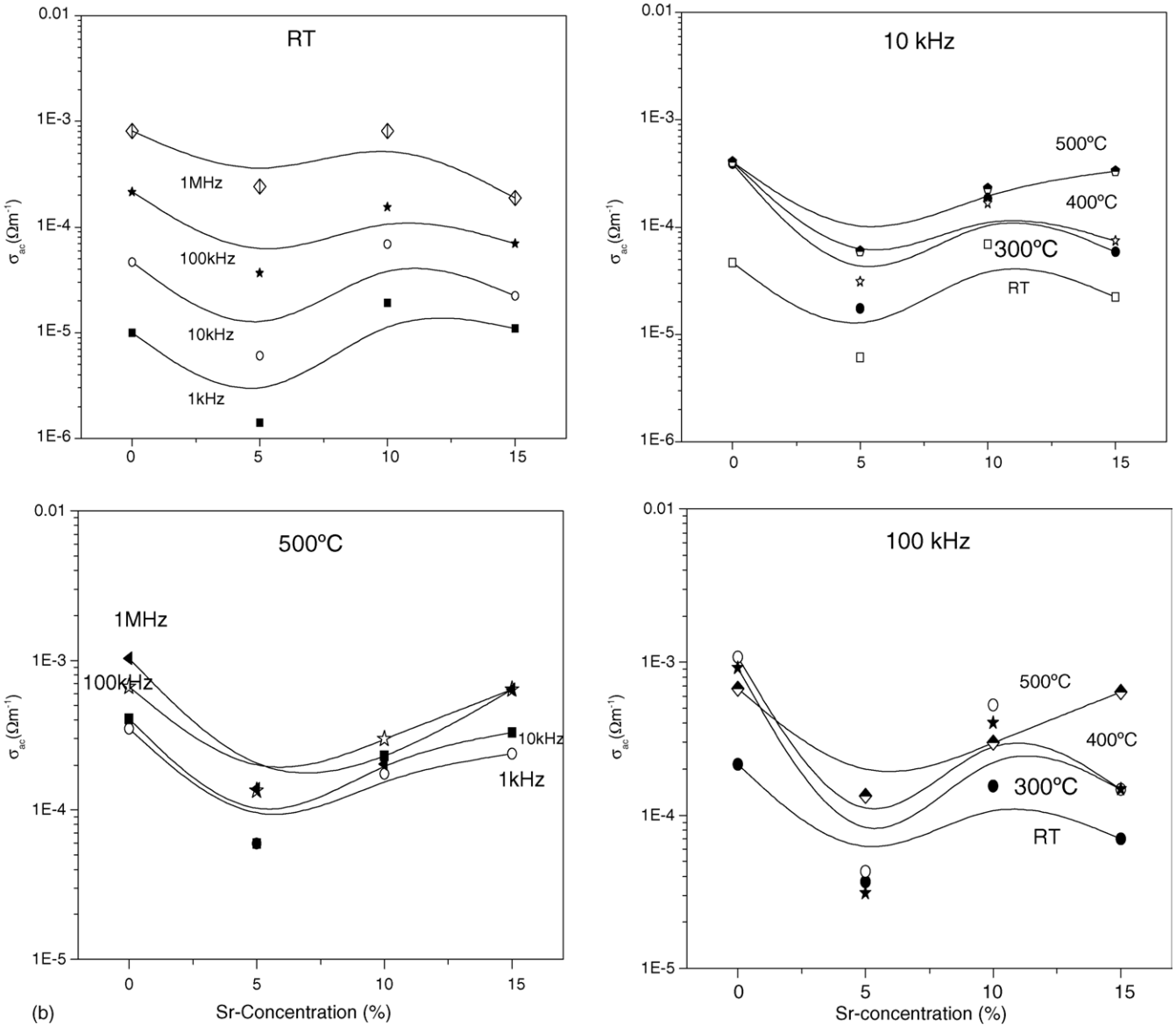

Fig. 5. (*Continued*).

at $x = 5\%$ may possibly be related to the enhancement in the barrier properties on Sr doping in good agreement with the observations from impedance analysis.

4. Conclusions

A new ceramic oxide, $Ba_{1-x}Sr_xSnO_3$, has been prepared by a high temperature solid-state reaction route. The formation of single-phase polycrystalline compound has been confirmed by XRD studies. Scanning electron microscopy has confirmed the polycrystalline texture of the material with porous microstructure. It has been observed that Sr substitution at the Ba-site has profound effect on the electrical behavior of the material. The complex impedance analysis has indicated lowering in the capacitance and enhancement of barrier properties evidenced by an increase in the net impedance of the material with Sr concentration when compared with that of the pure $BaSnO_3$. The enhancement in impedance with Sr substitution results in a corresponding decrease in the electrical conduction. The decrease in the electrical conductivity of Sr modified $BaSnO_3$ in comparison to pure $BaSnO_3$ has been interpreted to be due to the weakening in the capacitive (reactive) effects resulting in an enhancement of the bulk resistance on Sr substitution.

References

[1] J. Cerda, J. Arbiol, G. Dezanneau, R. Diaz, J.R. Morante, Synthesis of perovskite-type $BaSnO_3$ particles obtained by a new simple wet

chemical route based on a sol–gel process, Mater. Lett. 56 (2002) 131–136.
[2] J. Cerda, J. Arbiol, G. Dezanneau, R. Diaz, J.R. Morante, Perovskite-type $BaSnO_3$ powders for high temperature gas sensor applications, Sens. Actuators B84 (2002) 21–25.
[3] S. Upadhyaya, O. Prakash, D. Kumar, Solubility of lanthanum, nickel, and chromium in barium stannate, Mater. Lett. 49 (2001) 251.
[4] C.P. Udawatte, M. Kakihana, M. Yoshimura, Low temperature synthesis of pure and the (Ba_xSr_{1-x}) SnO_3 solid solution by the polymerized complex method, Solid State Ionics 128 (2000) 217–226.
[5] W. Lu, S. Jiang, D. Zhou, S. Gong, Structural and electrical properties of Ba (Sn, Sb) O3 electroceramics materials, Sens. Actuators 80 (2000) 35–37.
[6] A.-M. Azad, N.C. Hon, Characterization of $BaSnO_3$-based ceramics: part 1. Synthesis, processing and microstructural development, J. Alloys Comp. 270 (1988) 95–106.
[7] C.P. Udawatte, M. Kakihana, M. Yoshimura, Preparation of pure perovskite-type $BaSnO_3$ powders by the polymerized complex method at reduced temperature, Solid State Ionics 108 (1998) 23–30.
[8] V. Jayaraman, G. Mangamma, T. Gnanasekaran, G. Periaswami, Evaluation of $BaSnO_3$ in $Ba(Zr,Sn)O_3$ solid solutions as semiconductor sensor materials, Solid State Ionics 86–88 (1996) 1111–1114.
[9] O. Prakash, K.D. Mandal, C.C. Christopher, M.S. Sastry, D. Kumar, Preparation and characterization of strontium stannate-$SrSnO_3$, J. Mater. Sci. Lett. (1994) 1616–1617.
[10] L.-C. Tien, C.-C. Chou, D.-S. Tsai, Microstructure of Ba $(Mg_{1/2}Ta_{2/3})O_3$–$BaSnO_3$ microwave dielectrics, Ceram. Int. 26 (2000) 57–62.
[11] A.J. Moulson, J.M. Herbert, Electroceramics: Materials, Processing, Application, Champman and Hall, NY, 1990.
[12] R. Buchanan, Ceramic Materials for Electronics, Marcel Dekker, 1986.
[13] M.J. Madous, S.R. Morrison, Chemical Sensing with Solid State Devices, Acadmic Press, NY, 1989 (Chapter 3).
[14] T. Sato, Y. Bito, T. Murata, S. Ito, H. Matsuda, Y. Toyoguchi, Non aqueous electrolyte secondary battery, Japan Patent No. US 6423448, Matsushita Electric Industrial Co., Ltd.
[15] L. Shebanovs, X-ray studies of Debye temperature of some ABO_3 perovskites, Ferroelectrics 269 (2002) 87–92.
[16] W. Zheng, W. Pang, Key Lab. Inog. Hydrotherm. Synth. Wuji Cailiao Xuebao 11 (4) (1960) 740–744.
[17] I.R. Hines, N.L. Allan, R. Wendy, U.K. Flavell, J. Chem. Soc. Faraday Trans. 92 (12) (1996) 2057–2063.
[18] O. Prakash, D. Kumar, Dielectric relaxation and conduction in the system $Ba_{1-x}La_xSn_{1-x}Cr_xO_3$, J. Mater. Sci.: Mater. Electron. 12 (2000) 165–172.
[19] O. Prakash, D. Kumar, K.K. Shrivastava, R.K. Dwivedi, Electrical conduction behavior of cobalt substituted $BaSnO_3$, J. Mater. Sci. 36 (24) (2001) 5805.
[20] POWDMULT: An Interactive Powder Diffraction Data Interpretation and Indexing Program, Version 2.1, E.Wu, School of Physical Sciences, Flinder University of South Australia, Bradford Park, SA 5042, Australia.
[21] N. Dridi, A. Boukhari, J.M. Reau, E. Arbib, E.M. Holt, Crystal structure and ionic conductivity of crystalline and glassy $Na_2PbP_2O_7$, Solid State Ionics 127 (2000) 141.
[22] S. Selvasekarapandian, M. Vijaykumar, The ac impedance spectroscopy studies on $LiDyO_2$, Mater. Chem. Phys. 80 (2003) 29–30.